International Global Navigation Satellite Systems Association
IGNSS Symposium 2020

Colombo Theatres, Kensington Campus, UNSW Australia
5 – 7 February 2020

Spatiotemporal Correlation between Fault Tests Statistics in Integrated Time-Differenced Carrier Phase GPS Observations with INS

Ali Almagbile

Department of Geography, Yarmouk University, Irbid, Jordan
Tel:+962272111111 (3697),Fax: +96227211137
Email: a.magbile@yu.edu.jo

ABSTRACT

When high precision positioning is required, carrier phase observations are commonly fused with INS after fixing the ambiguity using differential technique. To overcome the drawbacks of double differencing, time-differenced carrier phase (TDCPH) observations technique are used. However, the positioning provided by (TDCPH) is still relative positioning because it is based on two consecutive epochs at the same satellite. As a result, if an outlier exists in a certain epoch, the following epoch will be inevitably influenced by this outlier. In this study, spatial and temporal (spatiotemporal) correlation between outlier tests is analysed. This has been performed under the presence of single and multiple outliers. The results show that when an outlier exists, many observations either in the same epoch or in the consecutive epoch particularly those which have strong correlation with outlier are influenced. The situation becomes more complicated when multiple outliers exist because all the combinations which have a common measurement with the outliers have large correlation and thus they are flagged as outliers.

KEYWORDS: Reliability theory, Correlation, Fault test, time-differenced Carrier phase, GPS/INS

1. INTRODUCTION

The integration of GPS/INS system is being intensively investigated as it can provide long-term high-accuracy and robust navigation solution. In normal operation, either GPS pseudorange or carrier phase observations are fused with INS to satisfy the requirements of different accuracy levels for various navigation applications. In some applications which

require meter-level accuracy, GPS pseudorange observations are preferably used. For high precision positioning, however, carrier phase observations are employed due to the fact that these observations have centimetres or even millimetres level accuracy. Therefore, double differencing carrier phase procedure is commonly utilized to achieve high precision positioning because it offers better eliminating common error sources across receiver and satellites, mitigate errors (eg., multipath and topographic) comparing with pseudorange observations.

The procedure of double differencing carrier phase requires the integer ambiguity resolution to achieve centimetre level positioning. With the LAMBDA (Least-squares AMBiguity Decorrelation Adjustment) method (De Jonge *et al*, 1996), the ambiguities are de-correlated to allow for efficient search for the integer candidate. Finally, a validation of the test is performed through using the ratio-test (Teunissen 2005, Feng *et al*, 2009). Although a high precision positioning can be obtained by the double differencing carrier phase, it is still suffering from several drawbacks such as delays that can disrupt real-time integer ambiguity resolution and the length of baseline. To overcome these limitations, time-differenced carrier phase observations technique was introduced. In this procedure, high precision navigation solution can be achieved as similar to those obtained by double differencing without being involved in the differential procedures (Farrel 2001, 2006, Han and Wang, 2012). The basic principle idea of time-differenced carrier phase is to subtract the carrier phase measurements at current epoch from the carrier phase measurements at the previous epoch. Thus, relative positioning can be obtained from two consecutive epochs at the same satellite (Almagbile, 2012).

Despite the fact that the time-differenced carrier phase technique offers high precision navigation solution, the obtained positioning by this technique is still a relative positioning (Han and Wang, 2012). This is because the positioning at current epoch is dependent on the previous epochs and thus they are physically correlated. In some situations when an outlier occurs at an epoch, the subsequent epochs will inherit all the deteriorations from the previous epochs which in turn cause unreliable positioning. In this case, the positioning in the influenced epoch will suffer from two main problems: the first problem is related to the original faulty observation which continuously occurs at the subsequent epochs due to the physical correlation. The other problem may arise due to the correlation between fault tests statistics at either the same epoch (spatial correlation) or subsequent epochs (temporal correlation). Consequently, many pure observations might be flagged as outliers while they are actually not.

Over decades, receiver autonomous integrity monitoring (RAIM) has been involved in enhancing the reliability and robustness of navigation solution. In this regard, Pseudorange-based RAIM (PRAIM) and Carrier-based RAIM (CRAIM) have been developed and applied in many applications. The CRAIM was designed for resolving ambiguity and validation, cycle slip detection, potential failures associated with differencing and correlation of errors (Feng *et al*, 2009). Nevertheless, the developed algorithms of RAIM are limited to detect and identify single fault at a time. In some occasions however, the performance of RAIM is degraded when the GPS observations are encountered multiple simultaneous faults. This situation is quite complicated comparing with the single fault case. This is because the faulty measurements may deteriorate almost all measurements particularly those which are strongly correlated with the faulty ones (Almagbile, 2019).

Early studies (e.g., Baarda 1967, 1968, Förstner, 1983, Teunissen, 1990) used the statistical

approaches for detecting and identifying outliers for different applications using Detection, Identification and Adaptation method (DIA). Then several studies (e.g., Knight *et al*, 2010, Almagbile *et al*, 2011, Wang *et al*, 2012, Yang *et al*, 2013) extended the theory for multiple outliers detection in integrated multi-sensor systems. Regardless the application types and the number of outliers, all studies in this direction used hypotheses testing for separating the outliers.

The current study employs the reliability theory for detection and identification single and multiple simultaneous faults in integrated GPS time-differenced carrier phase observations with INS. Correlation between fault test will be expanded from one-dimension to a multi-dimensional case to determine the influences of the faulty measurements on other pure observations. The multi-dimensional correlation will determine the relationships between a punch of measurements at spatial and temporal spaces. The outcomes of this study will provide a foundation for improving the quality control for time-differenced GPS carrier phase observations through checking potential faults in every observation spatially and temporarily. Once the identified outliers at a certain epoch are handled, the contamination will be avoided in the subsequent epochs.

The structure of this paper is as follows: Section 2 provides research methodology including a brief introduction about time-differenced carrier phase, Snapshot approach, multiple outliers detection and identification, and global correlation. Section 3 includes the test and results analysis followed by concluding remarks in Section 4.

2. METHODOLOGY

2.1 Time-Differenced Carrier Phase (TDCPH)

Time differenced carrier phase (TDCPH) approach has been employed to overcome the limitations associated with the differential technique. The limitations of differential technique are related to the cost of hardware used for collecting data, time consuming for fixing the ambiguities and validating the measurements, and selecting the suitable length of baseline between GNSS receivers (Almagbile, 2012). Thus, TDCPH technique allows getting high position accuracy by using the carrier phase measurements without being involved in differential techniques (Farrel, 2001, 2006).

The principle of TDCPH is based on subtracting the receiver coordinate at current epoch from previous epoch so that delta position can be obtained from two consecutive epochs in the same satellite (Wendel *et al*, 2006, Soon *et al*, 2008, Han and Wang, 2012). The mathematical representation can be found in Farrel (2001) and Han and Wang (2012).

2.2 Snapshot Approach

A tightly coupled integration of the time-differenced carrier phase observations (TDCPH) and INS was implemented using extended Kalman filtering. The Kalman filtering was then converted into Least Squares (Sorenson, 1970, Salzmann, 1993) to utilize the snapshot approach in detecting and identifying outliers in GPS/INS systems (Almagbile, 2019). This procedure is to detect and identify potential outliers in every measurement at every epoch.

Therefore, the Least Squares observation vector I_k is formed by integrating the Kalman filtering predicted states x_k and measurements vector z_k . This can be written mathematically as (Almagbile *et al*, 2010):

$$l_k = \begin{bmatrix} z_k \\ \bar{x}_k \end{bmatrix} \tag{1}$$

$$x_k = \Phi_{k-1} x_{k-1} + w_k \tag{2}$$

$$z_k = H_k x_k + v_k \tag{3}$$

where x_k is $(n\times 1)$ state vector, Φ_k is $(n\times n)$ transition matrix, z_k is $(r\times 1)$ observation vector, H_k is $(r\times n)$ observation matrix. The variables w_k and v_k are uncorrelated white noise errors with covariance matrices Q_k and R_k respectively. The design matrix A_k and the residual vector v_k can respectively be written as:

$$A_k = \begin{bmatrix} H_k \\ E \end{bmatrix}, v_k = \begin{bmatrix} v_{zk} \\ v_{\bar{x}k} \end{bmatrix} \tag{1}$$

The variance-covariance matrix Cl_k of Least Squares is derived from the measurement noise covariance matrix R_k and the predicted states covariance matrix $\bar{P}_k$ of Kalman filtering can be written as (Wang *et al*, 2012):

$$C_{l_k} = \begin{bmatrix} R_k & 0 \\ 0 & \bar{P}_k \end{bmatrix} = P^{-1} \tag{2}$$

where P is the weight matrix. The optimal estimate of the state parameters $\hat{x}_k$ and error covariance matrix $Q_{\bar{x}k}$ can be written as (Wang *et al*, 2013):

$$\hat{x}_k = (A_k^T P A_k)^{-1} A_k^T P l_k \tag{3}$$

$$Q_{\hat{x}_k} = (A_k^T P A_k)^{-1} \tag{4}$$

The residuals vector v_k and cofactor Q_{v_k} can be written as (Wang *et al*, 2012):

$$v_k = \begin{bmatrix} v_{zk} \\ v_{\bar{x}k} \end{bmatrix} = A_k \hat{x}_k - l_k \tag{5}$$

$$Q_{v_k} = Cl_k - A_k Q_{\hat{x}k} A_k^T \tag{6}$$

2.3 Identification of Multiple Outliers

Identifying multiple outliers in TDCPH observations can be performed by the following equation (Wang and Chen, 1999, Knight *et al*, 2010):

$$T_i^\theta = \frac{l^T PQ_v PG_i (G_i^T PQ_v PG_i)^{-1} G_i^T PQ_v Pl}{\sigma_0^2} \sim \chi^2_{1-\alpha_{T_i^\theta}} \qquad (10)$$

Where $\alpha_{T_i^\theta}$ is the level of significance for fault test, G is a $(n \times \theta)$ fault matrix, with rank θ, containing zeros with a one in each column corresponding to the number of faults in the observation vector. For instance, when two faults exist in the observations, G matrix will be formed as follows (Almagbile, 2019):

$$G = [g_i \quad g_j] \qquad (11)$$

$$g_i = [0 \quad 0 \quad 1 \quad . \quad . \quad 0]^T \qquad (12)$$

$$g_j = [0 \quad . \quad 0 \quad 0 \quad 1 \quad 0]^T \qquad (13)$$

where g_i and g_j are vectors can be used for different number of outliers. The T_i^θ is also $(n \times \theta)$ matrix corresponding to the G matrix. If the alternative hypothesis is accepted, the T_i^θ test statistics become non-central normal distribution and then the non-centrality parameter can be written as (Baarda, 1968**,** Wang and Chen, 1999):

$$\lambda = \frac{z^T G^T PQ_{vv} PGz}{\sigma_0^2} \qquad (14)$$

Where z is the true outlier vector, if the outlier identification is possible, the largest w_i^θ test is corresponding to the true outlier vector.

The minimal detection bias (MDB) can be determined using multiple correlation coefficients. MDB and multiple correlation can be written as follows (Knight *et al*, 2010):

$$P_{ij}^\theta = \sqrt{\frac{g_i^T PQ_{vv} PG_j (G_j^T PQ_{vv} PG_j)^{-1} G_j^T PQ_{vv} Pg_i}{g_i^T PQ_{vv} Pg_i}} \qquad (15)$$

With bounds of P_{ij}^θ are: $0 \leq P_{ij}^\theta \leq 1$

$$\nabla_0 S_i^\theta = \sqrt{\frac{\lambda \sigma_0^2}{g_i^T PQ_v Pg_i (1 - P_{ij}^\theta)}} \qquad (16)$$

2.4 Global Correlation Coefficient

In this study, the correlation between fault tests was designed as follows:

(1) Spatial correlation between fault tests to check the influences of outliers on other pure observations at the same epoch.

(2) Temporal correlation between two consecutive epochs to check the influences of the outliers on other pure observations at subsequent epochs.

The correlation coefficient can be used for single or multiple outliers. In any case, the dimension of the correlation should correspond to the number of outliers in the observations. Mathematically, this correlation can be written as follows (Li, 1986, Wang *et al*, 2013):

$$\left(Q_{ij}\right)_{Global} = \frac{tr(M_{ij})}{\sqrt{r_i . r_j}} \qquad (17)$$

Where $\left(Q_{ij}\right)_{Global}$ is the global correlation (Li, 1986), r_i and r_j are the degree of freedom for T_i^{θ} and T_j^{θ} respectively (Förstner, 1983).

$$M_{ij} = (P_{ii})^{-1}\left(P_{ij}\right)\left(P_{jj}\right)^{-1}\left(P_{ji}\right) \qquad (18)$$

$$P_{ij} = G_i^{\kappa} P Q_{vv} P G_j^{\theta} \qquad (19)$$

Where G_i^{θ} and G_j^{κ} are the same as in equations (11) and**,** θ and κ present the dimension of the correlation. The correlation dimension should coincide with the number of faults in the observations. Note that this correlation can be between observations at the same epoch (spatial) or between same observations at different epochs (temporal).

3. TEST AND RESULTS ANALYSIS

3.1 Test

Time-differenced carrier phase (TDCPH) GPS observations were fused with inertial navigation system (INS) using tightly coupled integration mode. One Leica 530 GPS receiver and one BEI C-MIGITSII (DQI-NP) INS unit were mounted on the top of land-based vehicle to collect dataset. Then raw GPS and INS data was fused using Kalman filtering with 24 error states. These states were divided into 9 states for the navigation solution (3 for each of position, velocity and attitude), 6 for INS accelerometers errors (bias and scale factor), 3 for gyro, 3 for gravity and the last 3 are allocated for lever arm errors.

The integration has been performed in a total of 649 epochs with different numbers of visible satellites. The number of tracked satellites was fluctuated around 7 satellites.

After performing the TDCPH/INS integration, outlier test was conducted based on the following scenarios:

- Scenario 1: epoch 10 was selected to simulate an outlier of 1 meter in the carrier phase

observations. Then the single outlier test was performed to identify the simulated outlier in this epoch using data snooping technique. This means that every carrier phase measurement is tested to check the ability of the test for truly identify the outlier. Then the correlation between outlier tests is performed.

- Scenario 2: two outliers of 1 and 0.5 meters are injected in measurement 1 and 3 at epoch 10 respectively. Then multiple fault test and multi-dimensional correlation were carried out to identify and separate the outliers.

3.2 Results

3.2.1 *Single outlier test*

The performance of outlier test has been examined for truly detecting and identifying single outlier. The results have been depicted in Table 1 and also visualised in Figure 1. When a single outlier exists in the observations, the outlier test is able to identify the contaminated measurement because its value exceeds the critical value (10.82). In order to illustrate the performance of the test, the outlier test is conducted before and after injecting an outlier in the observation number one. As it can be noted, the observation number one has the largest value among all the observations at epoch 10. The outlier test value for this observation was increased from 0.046 centimetres to more than 60.3 meters. Moreover, other observations were adversely influenced by this outlier. As an example, the outlier test value for the observation number two has jumped from 0.012 centimetres to around 5.3 meters. The values of the minimal detectable bias (MDB) are fluctuated between 0.95 to 0.42 centimetres. This emphasis that since the injected outlier is larger than the MDB value, the test is able to detect the outlier and vice versa.

Since Time-differenced observations were fused with INS, the influence of outlier will inevitably transfer with time. This situation can be seen in the observation number one at epoch 11. This observation is considered outlier because its value is larger than the critical value. In addition, the values of outlier test for other observations at epoch 11 were also increased. Due to the high precision observations, The MDB values at epoch 11 are slightly different from those at epoch 10.

Epoch 10			***Epoch 11***		
Test without fault	***Test with a fault of 1 meter in measurement 1***	***MDB***	***Test without fault***	***Influenced measurements***	***MDB***
0.046	60.354	0.766663	0.003	33.939	0.766609
0.012	5.317	0.423993	0.006	0.471	0.423989
0.313	3.314	0.532763	0.446	1.039	0.532713
0.576	0.060	0.510700	0.468	1.793	0.510733
0.654	0.008	0.526443	0.514	2.691	0.526457
0.001	0.443	0.428642	0.009	0.563	0.428642
0.006	0.600	0.470857	0.002	1.164	0.470854
0.335	0.117	0.951863	1.860	2.686	0.952017

Table 1. Fault test at epoch 10 and 11 with MDB

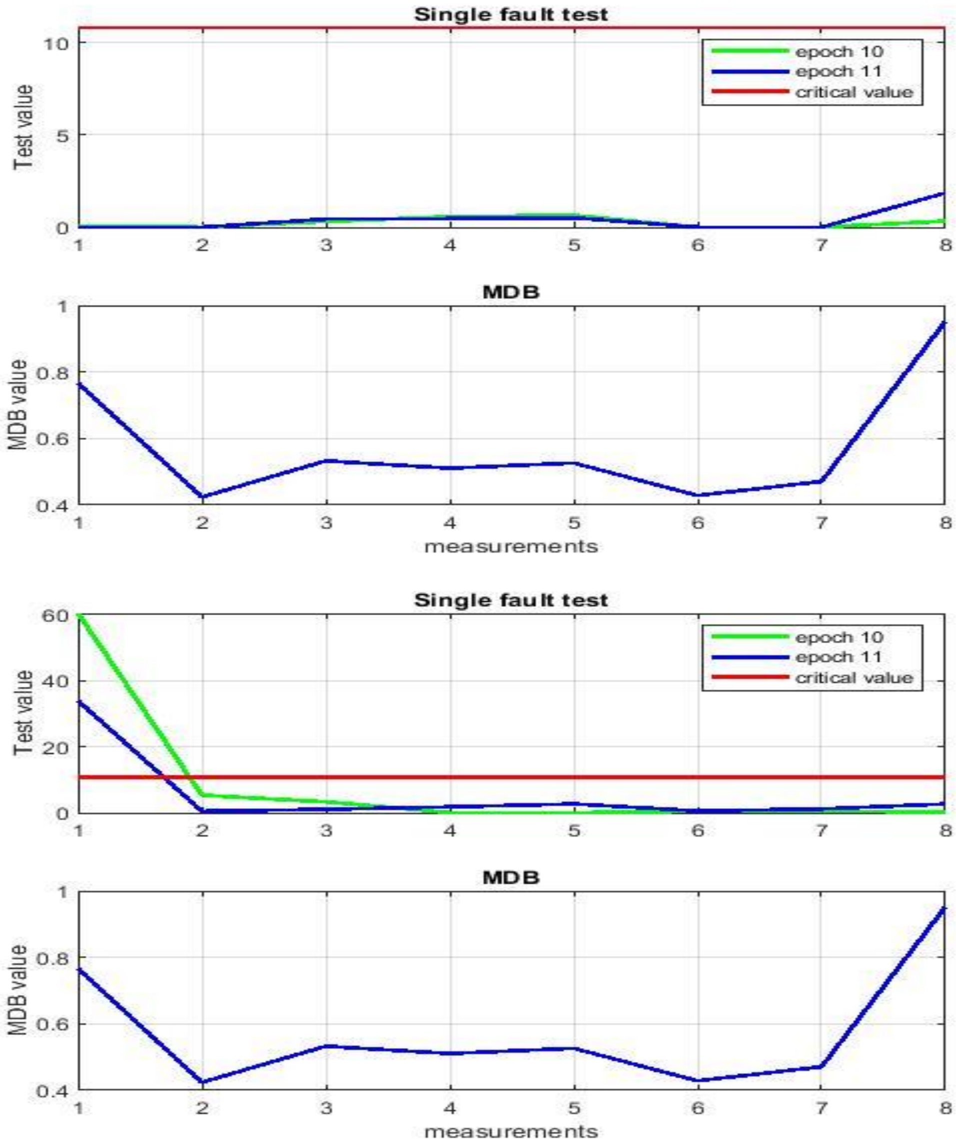

Figure 1. Single outlier test and MDB at epoch 10 and 11, without fault (up), with a fault of I meter in the measurement 1 (bottom)

One can note that the value of outlier test has changed spatially and temporally. The spatial changes mean each observation at the same epoch has different values, whereas temporally is different values for the same observation at different epochs. The spatial and temporal variations of outlier test value are resultant from the correlation coefficient (Table 2). This correlation indicates the degree of the relationship between the observations, thus high correlation between observations means they are very sensitive to changes in any observations. From Table 2 one can see that when the correlation is high, the outlier test value is high too. Since the difference between epoch 10 and 11 is tiny, the spatial and temporal correlation values are almost the same.

p_{ij}		Epoch 10								Epoch 11							
		1	2	3	4	5	6	7	8	1+	2+	3+	4+	5+	6+	7+	8+
Epoch 10	1	1.00	0.20	0.79	0.17	0.28	0.31	0.34	0.55	1.00	0.20	0.79	0.17	0.28	0.31	0.34	0.55
	2		1.00	0.02	0.12	0.14	0.05	0.11	0.17	0.20	1.00	0.02	0.12	0.14	0.05	0.11	0.17
	3			1.00	0.40	0.40	0.11	0.00	0.01	0.79	0.02	1.00	0.40	0.40	0.11	0.00	0.01
	4				1.00	0.57	0.01	0.15	0.17	0.17	0.12	0.40	1.00	0.57	0.01	0.15	0.17
	5					1.00	0.03	0.18	0.21	0.28	0.14	0.40	0.57	1.00	0.03	0.18	0.21
	6						1.00	0.13	0.32	0.31	0.05	0.11	0.01	0.03	1.00	0.13	0.32
	7							1.00	0.85	0.34	0.11	0.00	0.15	0.18	0.13	1.00	0.85
	8								1.00	0.55	0.17	0.01	0.17	0.21	0.32	0.85	1.00
Epoch 11	1+									1.00	0.20	0.79	0.17	0.28	0.31	0.34	0.55
	2+										1.00	0.02	0.12	0.14	0.05	0.11	0.17
	3+											1.00	0.40	0.40	0.11	0.00	0.01
	4+												1.00	0.57	0.01	0.15	0.17
	5+													1.00	0.03	0.18	0.21
	6+														1.00	0.13	0.32
	7+															1.00	0.85
	8+																1.00

Table 2. Spatial and temporal correlation under the presence of single outlier at epoch 10 (plus sign means the subsequent epoch)

3.2.2 Multiple outliers test

Under the presence of two outliers, the test is conducted to determine its ability for identifying multiple outliers. As shown in Figure 2, the test was conducted before and after injecting two outliers in the observation number 1 and 3. Without outliers, the test values for all the measurement combinations were less than the critical value (13.83). However, when two outliers exist in the observations, the test identifies observation 1 and 3 as outliers. This situation can be seen at both epochs. As mentioned above, due to the correlation between the observations, other measurement combinations such as (1, 4), (1, 6) and (1, 8) are considered outliers at both epochs. The MDB values ranges between 0.5 to around 1.8 meters and these values are almost the same at both epochs.

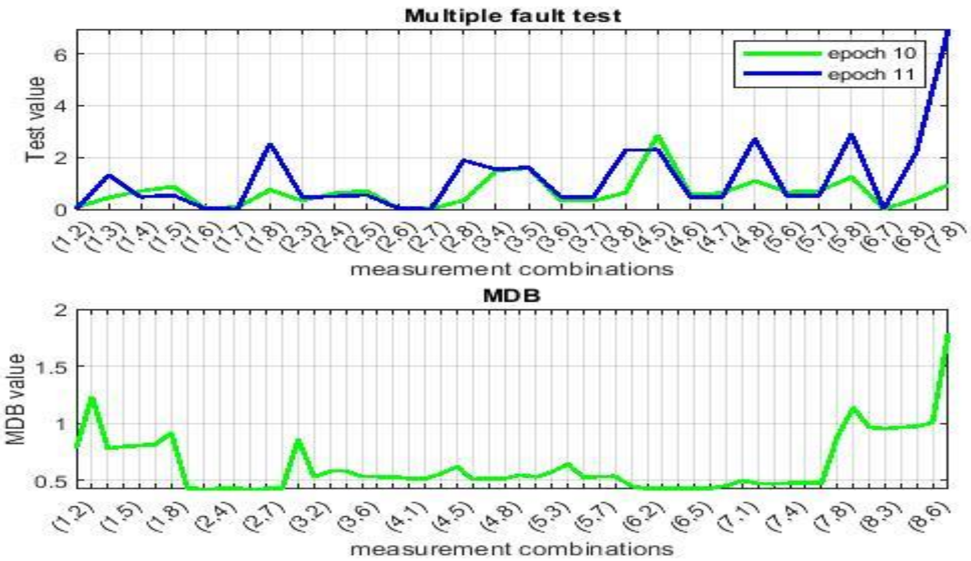

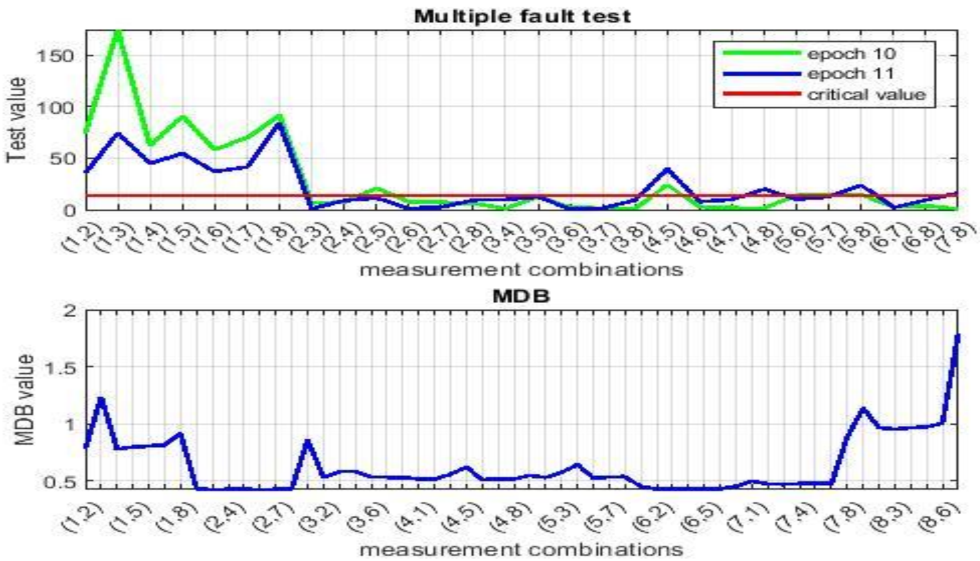

Figure 2. Multiple outlier test and MDB at epoch 10 and 11, without fault (up), with two faults in measurement 1 and 3 (bottom)

3.2.3 Detailed analysis of spatial and temporal (spatiotemporal) correlation

Figure 3 depicts three cases of correlation when multiple outliers exist in the observations. These cases can be summarized as follows:

- Case 1: spatial correlation between the measurement pair (1, 3) and all the measurement combinations at epoch 10 (Figure 3 (up))
- Case 2: spatial and temporal correlation between the measurement pair (1, 3) at epoch 10 and all the measurement combinations at epoch 11 (Figure 3 (middle))
- Case 3: spatial and temporal correlation between the measurement pair (1, 3) at epoch 10 and hybrid measurement combinations. The hybrid measurement combinations include single measurement from epoch 10 and single measurement from epoch 11. For example, a combination contains measurement 2 from epoch 10 and measurement 3 from epoch 11 (2, 3+) (Figure 3 (bottom))

In the first case, it can be seen that all of the combinations which includes either 1 or 3 have the largest correlation with the pair (1, 3). For instance, the measurement combinations (1, 2), (1, 4), (3, 6) and (3, 8) have large correlation comparing with the combinations (2, 4), (2, 6), (5, 6) and (6, 7). Similar situation can be found in the second case. In the third case, two combinations namely (1, 3+) and (3, 1+) have full correlation with the pair (1, 3) because they are correlated with themselves even though they belong to different epoch. Other combinations such as (1, 5+), (1, 7+), (3, 4+) and (3, 8+) have the largest correlation, whereas the smallest correlation occurs in the combinations (2, 5+), (5, 5+), (6, 7+) and (7, 7+). The largest correlation occurs because of a common observation with the pair (1, 3).

As a result of the above analysis, when two outliers exist in the observations, it can be very complicated scenario because they deteriorate almost all of the combinations which have a common measurement with the outliers. In addition to that, the existing of outliers in a certain epoch will inevitably influence the observations in the subsequent epoch due to the high correlation between them.

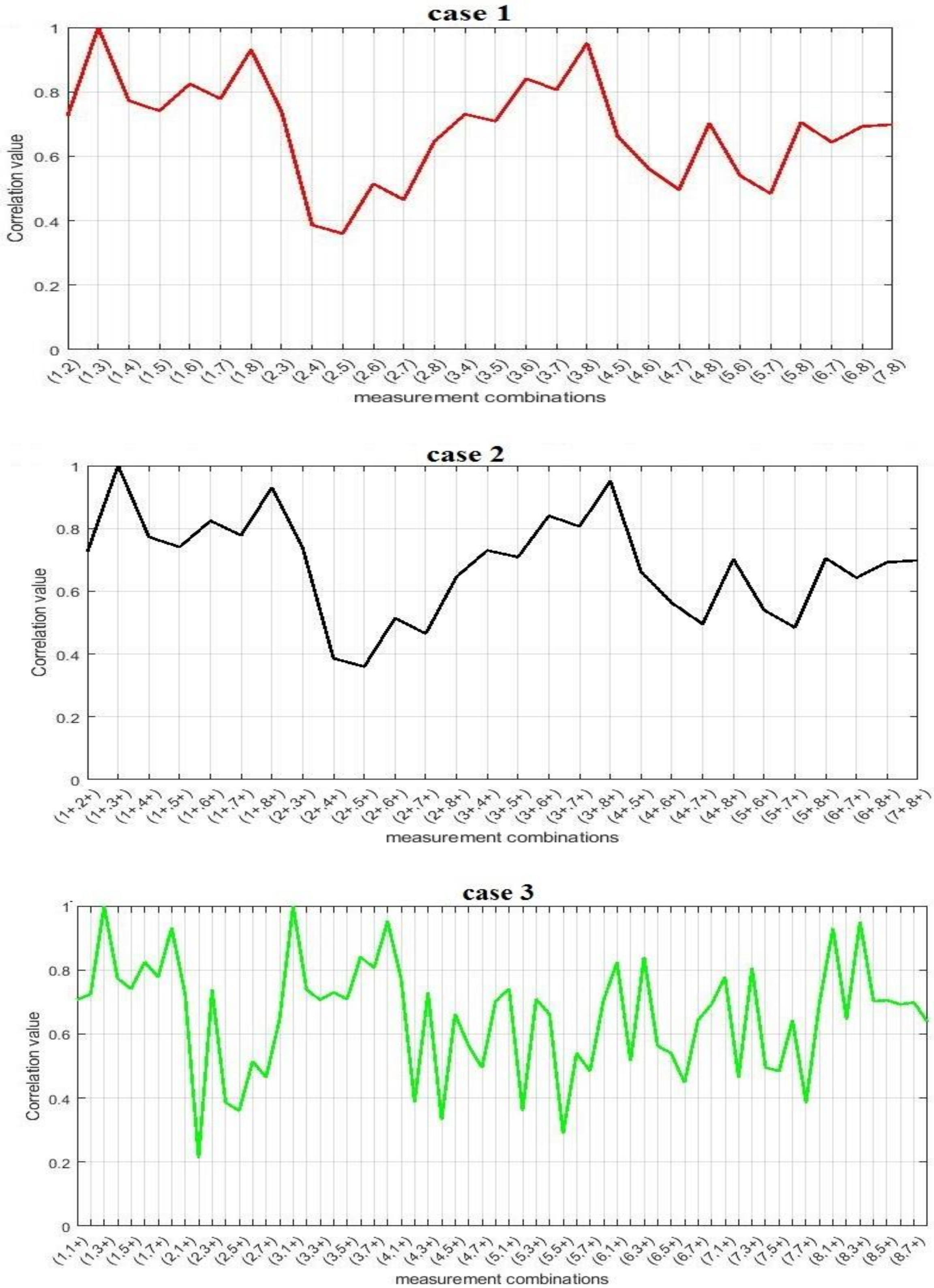

Figure 3. Spatial correlation between measurement pair (1, 3) and all measurement combinations at epoch 10 (up), spatial correlation between all measurement combinations at epoch 11(middle), temporal correlation between measurement pair (1, 3) at epoch 10 and all measurement combinations at epoch 11 (bottom) under the presence of two faults

4. CONCLUSIONS

Under the presence of single and multiple outliers in the integrated time-differenced GPS carrier phase observations and INS, this study investigates spatial and temporal correlation. Existing single or multiple outliers in the measurement leads to deteriorate other observations due to the correlation coefficient. If the influence of outliers is within the same epoch, a spatial correlation indicates the degree of effect. However, when time-differenced observations are fused with INS, the influence of outliers will transfer to the subsequent epochs due to the physical correlation. When outliers exist in two consecutive epochs, temporal correlation can be employed to control the influence of outliers.

In case of single outlier, the spatiotemporal correlation provides a clear indication of the probability of separation between the true outlier and the influenced observations. For multiple fault case, the situation becomes more complicated to separate the actual outliers from the influenced observations. This is because all the measurement combinations which have a common measurement with the outliers are flagged as outliers. This has been shown when using spatiotemporal correlation under the presence of two outliers in the measurements.

Further analysis of the spatiotemporal correlation when multiple outliers exist in single and multiple epochs is recommended for the future research.

REFERENCES

Almagbile A, Wang J, Ding W (2010) Evaluating the performance of adaptive Kalman filter methods in GPS/INS integration. *Journal of Global Positioning Systems*, 9, 33–40

Almagbile A, Wang J (2011) Analysis of outlier separability in integrated GPS/INS systems. *IGNSS symp*. Sydney Australia 15-17 November.

Almagbile A (2012) GNSS/INS Integration for Positioning and Navigation: Modelling and Quality Analysis, *PhD thesis*, UNSW, Australia

Almagbile A, (2019). Geometric and statistical interpretation of correlation between fault tests in integrated GPS/INS systems. *Journal of Applied Geodesy*, 13(3), pp. 267-278.

Baarda W (1967) Statistical concepts in geodesy, *Netherlands Geodetic, Commission, Publications on Geodesy*, New Series 2, No. 4, Delft (ISBN-13: 9789061322085, ISBN-10: 9061322081)

Baarda W (1968) A testing procedure for use in geodetic networks *Netherland Geodetic Commission*, vol 2, issue 5 (ISBN-13: 9789061322092, ISBN-10: 906132209X)

De Jonge P, Tiberius C (1996) The LAMBDA method for integer ambiguity estimation: implementation aspects. *Tech Rep. 12, Delft Geodetic Computing Centre*, IGR-series

Farrell JL (2001) Carrier phase processing without integers, *ION 57th Annual Meeting*, Albuquerque, NM, USA

Farrell JL (2006) Velocity and acceleration from unaided carrier phase, *IEEE/ION PLANS* 2006, Coronado, CA, USA

Feng S, Ochieng W, Moore T, Hill C, Hide C (2009) Carrier Phase-Based Integrity Monitoring for High-Accuracy Positioning, *GPS Solutions* 13 (1), 13-22.

Förstner W (1983) Reliability and discernability of extended Gauss-Markov models. In: Seminar on mathematical models to outliers and systematic errors, *Deutsche Geodätische Kommision*, Series A, no. 98. Munich, Germany, pp 79–103 (ISSN 978376681802)

Han S, and Wang J (2012) Integrated GPS/INS navigation system with dual-rate Kalman Filter, *GPS Solutions*, 16, 389–404

Knight NL,Wang J, Rizos C (2010) Generalized measures of reliability for multiple outliers, *Journal of Geodesy*, 84:625–635

Li DR (1986) Trennbarkeit und Zuverlässigkeit bei zwei verschiedenen alternativhypothesen im Gauß–Markoff-Modell, vol 3. Zeitschrift für Vermessungswesen, Heft

Salzmann M (1993) Least squares Filtering and Testing for Geodetic Navigation Applications, Netherlands Geodetic Commission, *publications on Geodesy*, New Series, Delft, The Netherlands, No. 37, 209 pp.

Soon K H, Scheding S, Lee HK, Lee HK, Durrant-Whyte, H (2008) An Approach to Aid INS Using Time Differenced GPS Carrier Phase (TDCP) Measurements, *GPS Solution*, Vol. 12, pp. 261-271

Sorenson H W (1970) Least Squares Estimation: from Gauss to Kalman, *IEEE Spectrum*, Vol. 7, pp. 63-68

Teunissen PJG (2005) Integer aperture bootstrapping: a new GNSS ambiguity estimator with controllable fail-rate. *Journal of Geodesy*, 79(6– 7):389–397

Teunissen PJG (1990) An integrity and quality control procedure for use in multi sensor integration. In: *Proceedings ION GPS* (republished in ION Red Book Series, vol. 7, 2010)

Wendel J, Meister O, Moenikes R, Trommer GF (2006) Time-Differenced Carrier Phase Measurements for Tightly Coupled GPS/INS Integration, *PLANS 2006*, San Diego CA, pp. 54-60.

Wang J, Chen Y (1999) Outlier detection and reliability measures for singular adjustment models, *Geomat Res Aust* 71:57–72

Wang J, Almagbile A, Wu Y, Tsujii T (2012) Correlation Analysis for Fault Detection Statistics in Integrated GNSS/INS Systems, *Journal of Global Positioning Systems*, 11(2), pp. 89-99

Wang J, Wu Y, Alqurashi M (2013) Separability analysis for multiple faults in GNSS/INS integration. In: *Proceedings of the international GNSS society symposium*, Gold coast, Australia

Yang, L, Wang J, Knight N, Shen Y (2013) Outlier separability analysis with a multiple alternative hypotheses test, *Journal of Geodesy*, 87, 591-604.